Published in final edited form as:

Osteoarthritis Cartilage. 2017 May ; 25(5): 676–684. doi:10.1016/j.joca.2016.11.016.

Patient-specific Chondrolabral Contact Mechanics in Patients with Acetabular Dysplasia Following Treatment with Peri-acetabular Osteotomy

Christine L. Abraham[1,2], **Spencer J. Knight**[1], **Christopher L. Peters**[1,2], **Jeffrey A. Weiss**[1,2,3], and **Andrew E. Anderson**[1,2,3,4,*]

[1]Department of Orthopaedics, University of Utah, 590 Wakara Way, Salt Lake City, UT, 84108, USA

[2]Department of Bioengineering, University of Utah, James LeVoy Sorenson Molecular Biotechnology Building, 36 S. Wasatch Drive, Rm. 3100, Salt Lake City, UT 84112 USA

[3]Scientific Computing and Imaging Institute, 72 S Central Campus Drive, Room 3750, Salt Lake City, UT 84112, USA

[4]Department of Physical Therapy, University of Utah, 520 Wakara Way, Suite 240 Salt Lake City, UT 84108, USA

Abstract

OBJECTIVE: Using a validated, patient-specific finite element (FE) modeling protocol, we evaluated cartilage and labrum (i.e. chondrolabral) mechanics before and after peri-acetabular osteotomy (PAO) to provide insight into the ability of this procedure to improve mechanics in dysplastic hips.

DESIGN: Five patients with acetabular dysplasia were recruited in this case-controlled, prospective study. Models, which included anatomy for bone, cartilage, and labrum, were generated from computed tomography arthrography scans acquired before and after PAO. Cartilage and labrum contact stress and contact area were quantified overall and regionally. Load supported by the labrum, expressed as a percentage of the total hip force, was analyzed.

RESULTS: Percent cartilage contact area increased post-operatively overall, medially, and superiorly. Peak acetabular contact stress decreased overall, laterally, anteriorly, and superiorly. Average contact stress decreased overall, laterally, anteriorly, and posteriorly. Only average contact

[*]**Correspondence address:**Andrew E. Anderson, PhD, University of Utah, Department of Orthopaedics, Harold K. Dunn Orthopaedic Research Laboratory, 590 Wakara Way, Salt Lake City, UT 84108, +1 801 587-5208, andrew.anderson@hsc.utah.edu.

Author Contributions

CLA: contributed to the design of the study, recruited patients, segmented images, generated FE models, post-processed data, performed the statistics, interpreted study results, and drafted the manuscript. SJK: segmented images, generated FE models, post-processed data, and edited the manuscript. CLP: contributed to the design of the study, assisted with clinical interpretation, and edited the manuscript. JAW: contributed to the design of the study, interpreted study results, and edited the manuscript. AEA: designed the study, supervised the study, reviewed the results for accuracy, assisted with clinical interpretation, and edited the manuscript. CLA and AEA take responsibility for the integrity of this work.

Competing Interest Statement

The authors have no conflicts of interest.

stress on the superior labrum and peak labrum stress overall decreased. Load supported by the labrum did not change significantly.

CONCLUSIONS: PAO was efficacious at medializing cartilage contact and reducing cartilage contact stresses, and therefore may minimize deleterious loading to focal cartilage lesions, subchondral cysts, and cartilage delaminations often observed in the lateral acetabulum of dysplastic hips. However, the excessively prominent, hypertrophied labrum of dysplastic hips remains in contact with the femoral head, which continues to load the labrum following PAO.The clinical ramifications of continued labral loading following PAO are not known. However, it is plausible that failure to reduce the load experienced by the labrum could result in end-stage hip OA following PAO.

Keywords

hip; cartilage; labrum; acetabular dysplasia; peri-acetabular osteotomy; finite element modeling

Introduction

The etiology of hip osteoarthritis is multifactorial; both whole-body-level factors (e.g. race, diet, weight, sex, genetics) and joint-level factors (e.g. joint morphology, muscle function) are involved [1]. Nevertheless, most cases of hip OA occur secondary to untreated anatomical deformities, such as acetabular dysplasia and femoroacetabular impingement [1]. There is some disagreement as to which percentage of hip OA cases can be attributed to each deformity. For example, investigators have estimated dysplasia accounts for 50% of hip OA cases [2, 3], whereas femoroacetabular impingement has been suggested to be more common, being observed in 80% of cases [4]. Regardless, it is generally agreed that hip OA develops in these hips as a result of abnormal cartilage and labrum (i.e. chondrolabral) mechanics, which induce structural failure and a cascade of molecular and inflammatory responses that typify hip OA [1, 5].

In dysplastic hips, the acetabulum is shallow, resulting in a joint with inadequate femoral head coverage [6, 7]. Reduced coverage in dysplastic hips is hypothesized to cause chronic overload of cartilage, resulting in end-stage OA [8, 9]. Periacetabular osteotomy (PAO) aims to prevent OA by reorienting the acetabulum into a position that increases anterolateral coverage [8, 10, 11]. Medialization of the joint may reduce cartilage stresses along the lateral border of the acetabulum, which is important as many dysplastic hips have cartilage lesions in this region [12]. PAO may also reduce load and stress at the labrum. Normalization of labral mechanics may be critical: recent finite element (FE) modeling research suggests that it is the labrum that may initially experience stress overload in pre-osteoarthritic hips with dysplasia, rather than cartilage, which may lead to an out-to-in progression of OA [13, 14].

Clinical studies have demonstrated positive outcomes after PAO [15–17], but 40% of these patients eventually require hip arthroplasty [18]. Measurements of chondrolabral mechanics, including quantification of stress, contact area, and load sharing, before and after PAO, would establish the biomechanical efficacy of this procedure. Chondrolabral mechanics cannot be measured in-vivo, but they can be predicted from FE models [19, 20]. Generating

three-dimensional (3D) reconstructions of bone, cartilage, and labrum from medical images to serve as FE model geometry is time-consuming [21]. Thus, hip FE models have often assumed constant thickness for cartilage and concentric bone and cartilage [9, 22]. Unfortunately, these simplifications yield unrealistic predictions [23, 24]. More recent FE models of native hips include cartilage thickness [13, 14, 19, 20, 25–27], but most of these models neglect the labrum. Importantly, simulations that analyzed hip mechanics before and after PAO excluded the labrum and did not incorporate spatially varying cartilage thickness [22, 28].

The objective of this study was to predict chondrolabral mechanics before and after PAO using FE models that included patient-specific anatomy. We hypothesized that PAO would: 1) medialize cartilage contact stresses and reduce average and peak cartilage contact stress, and 2) reduce peak and average stress, contact area, as well as load to the labrum.

Methods

Patient Recruitment, Radiographic Evaluation, CT Arthrography

All research was performed in accordance with the Helsinki Declaration with informed consent and institutional board approval. Patient demographics were reported as the mean ± standard deviation. Five patients with acetabular dysplasia (1 male and 4 female) aged 29.8 ± 5.8 years and with a body mass index (BMI) of 21.1 ± 3.6 $kg•m^{-2}$ underwent PAO by a single surgeon (author CLP) with 20 years of experience managing dysplasia. Each patient was imaged using radiographs and computed tomography (CT) arthrography before and after surgery, at minimum 1 year follow-up (19.3 ± 7.2 months, yielding a post-operative age of 31.5 ± 6.3 years). BMI following surgery was 21.4 ± 2.9 $kg•m^{-2}$. Anteroposterior radiographs evaluated morphology in pre- and post-operative states.

A previously described CT arthrogram protocol [26] was performed to visualize, within a single image sequence, opposing layers of cartilage, the labrum, cortical bone, and trabecular bone. Images were acquired with a 128-section single-source CT scanner (SOMATOM Definition™; Siemens Healthcare) with the following settings: 120 kVp, 100–400 mAs, 512 × 512 matrix, 1.0 pitch, 300–400 mm FOV, and 0.7 mm slice thickness. A Hare traction splint was applied during the CT scan to ensure that contrast agent imbibed the joint space [26].

FE Model Generation

FE models were generated from the CT images using a validated protocol [19, 20]. Briefly, CT images were up-sampled to three times their native resolution to reduce stair-case artifact in 3D reconstructions [25]. The CT images were then segmented semi-automatically using commercial software (Amira, v6.0, FEI, Hillsboro, OR) to generate 3D reconstructions of trabecular bone, cortical bone, pelvic and femoral cartilage, and the acetabular labrum.

The three-dimensional reconstructions were smoothed, decimated and discretized into FE meshes (Fig. 1). Here, cortical bone was represented as triangular shell elements with position- dependent thickness, calculated as the geometric distance between the inner and outer cortex [19]. Pelvic and femoral cartilage as well as the acetabular labrum was

represented as hexahedral elements [13, 19, 25, 27]. The boundary between cartilage and labrum was assumed to be located where the concave acetabulum transitioned into the convex acetabular rim [13, 14]. Element densities were based on previous mesh convergence analyses [19].

Constitutive models for bone, cartilage, and labrum followed other FE studies of the hip [14, 19, 25]. Here, bone was represented as isotropic linear elastic (E = 17 GPa, ν = 0.29) [31]. Cartilage was represented as a nearly incompressible, neo-Hookean hyperelastic material (G = 13.6 MPa, K = 1359 MPa) [19, 32]. The labrum was represented as transversely isotropic hyperelastic [34] with material coefficients (C_1 = 1.4 MPa, C_3 = 0.005 MPa, C_4 = 36, C_5 = 66 MPa, λ^* = 1.103) derived from experimental data of bovine tissue [35]. Here, C_1 referenced the shear modulus; equations describing the behavior of the fibers included material coefficients that scaled the exponential stress (C_3), specified the rate of collagen uncramping (C_4), the modulus of straightened collagen (C_5), and the stretch at which collagen straightened (λ^*)

A range of anatomical positions and loads, expressed in percent body-weight (BW), were applied to each FE model to analyze activities encountered during daily life. These included walking at toe-off (WTO, 205% BW), midstance during walking (WM 203% BW), the transition of heel-strike and midstance for stair descent (DHM 230% BW), and heel-strike during stair ascent (AH, 252% BW) using the Bergmann dataset [36]. During loading, the pubis and sacroiliac joint were held fixed, but the remaining hemipelvis and femur were free to deform. The femur was translated along the loading axis until the desired load was achieved, but was free to translate in the plane normal to the loading axis to achieve equilibrium [13, 25, 27]. Tied and sliding contact definitions followed previous FE studies [13, 14]. All FE models were analyzed with NIKE3D [37].

Measures of Chondrolabral Mechanics

Peak and average contact stress and contact area were recorded on the surface of the acetabular cartilage and labrum. Only those FE nodes in contact (i.e. > 0.0 MPa) were considered in the calculation of the average stress. The load supported by the labrum was reported as a percentage of the total force transferred across the hip. Contact stress and contact area were evaluated in the lateral and medial regions (Fig. 2-A), and in the anterior, superior, and posterior regions (Fig. 2-B). Contact area was presented as a percentage of the total surface area of acetabular cartilage. Fringe plots of contact stress for each subject and activity were generated. Similar plots were created to visualize average stresses at each FE mesh node for the acetabular cartilage. The same number of node and elements were used to represent acetabular cartilage across subjects; nodal connectivity was also preserved across subjects. This one-to-one correspondence made it straightforward to average nodal stresses. However, it was necessary to select a representative mesh to visualize average nodal stress. To select the representative mesh, the articulating surface of acetabular cartilage from each patient mesh was fit to a sphere. Next, the average radius of the sphere fit for subjects was calculated. The single patient-specific mesh that had a radius closest to the average radius was designated as the representative mesh. Nodal contact stress values of all subjects were

mapped onto this representative mesh, and then averaged. Pre- and post-processing was performed using PreView and PostView, respectively [38].

Statistical Analysis

All paired-sample differences between pre- and post-operative states within the same patients were assessed statistically using a mixed-effects linear regression, where activities were nested within patients. Changes in peak and average contact stress, and percent contact area were analyzed for all activities as a function of region. Load to the labrum was represented as a single value. Finner's procedure corrected for multiple comparisons [39]. Here, we adjusted for two comparisons when displaying results for medial and lateral regions, and three comparisons when displaying results for anterior, posterior, and superior regions. Mixed-effects linear regression analyzes and reports the difference between two measures, not the discrete value, to ascertain if they are significant. Thus, where appropriate, the discrete values for each metric (e.g. average and peak contact stress) were reported in addition to a 95% confidence interval (CI) of the mean differences between pre- and post-operative states. All statistical analyses were performed in Stata (v13.0, StataCorp LP, College Station, TX), with plots generated using SigmaPlot (v11.0; Systat Software, San Jose, CA). Significance for all tests was set at $P \leq 0.05$.

Results

Radiographic Measurements

In the pre-operative state, the CEA was 11.7 ± 4.3 degrees, with an acetabular index of 23.7 ± 9.6 degrees. Following surgery, the lateral CEA was increased to 30.2 ± 4.1 degrees and acetabular index decreased to 8.8 ± 4.9 degrees.

Acetabular Cartilage Contact Patterns

Contact patterns for all patients were bicentric pre- and post-operatively (Fig. 3). However, contact stresses appeared more focal in the pre-operative state (Fig. 3). When mapped to the representative mesh, the lateral regions and anterolateral rim in the pre-operative state exhibited concentrated regions of elevated contact stress (Fig. 4). Post-operatively, contact shifted medially and demonstrated loading primarily in the superomedial acetabulum for all activities, with stresses distributed in more regions of the acetabulum (Fig. 4).

Acetabular Cartilage Peak and Average Contact Stress

Total peak acetabular cartilage contact stress significantly decreased from 20.0 MPa pre- to 13.3 MPa post-operatively across all activities and all patients (−6.7 MPa, 95% CI: −9.2, −4.3 MPa, $P<0.001$) (Fig. 5-A). Total average contact stress significantly decreased from 4.3 MPa pre- to 3.7 MPa post-operatively across all activities and all patients (−0.6 MPa, 95% CI: −1.0, −0.3 MPa, $P<0.001$) (Fig. 5-B). When partitioned into lateral and medial regions, a significant decrease in peak and average contact stress in the lateral region was observed post-operatively ($P<0.001$ for both) (Fig. 5-A, 5-B). Conversely, average contact stress significantly increased medially ($P=0.003$); peak contact stress trended towards a significant increase medially ($P=0.071$) (Fig. 5-A, 5-B). Peak contact stress was significantly smaller post-operatively in the anterior and superior regions; a trend towards a significant decrease

was observed posteriorly (P=<0.001, 0.012, 0.057 for anterior, superior, posterior, respectively) (Fig. 5-A). Average contact stress significantly decreased post-operatively in the anterior and posterior regions (P=0.001, 0.037, respectively) (Fig. 5-B).

Acetabular Cartilage Percent Contact Area

The total percent of acetabular cartilage in contact increased significantly post- operatively across all activities from 20.4% before to 24.3% after surgery (3.9%, 95% CI: 1.0, 6.7%, P=0.008) (Fig. 5-C). By region, percent contact increased significantly medially and superiorly across all activities (P<0.001 for both) (Fig. 5-C).

Labral Contact Stress, Contact Area, Load Supported

Considering the total surface, peak contact stress on the labrum was significantly reduced from 14.9 MPa before surgery to 11.1 MPa after (−3.8 MPa, 95% CI: −6.97, −0.55 MPa, P=0.022). However, there were no significant changes in the anterior, superior, or posterior regions (P=0.118, 0.451, 0.118, respectively). Considering all activities, average contact stress was significantly reduced from 2.4 MPa pre- to 1.8 MPa post-operatively on the superior labrum (Fig. 6-A) (−0.6 MPa, 95% CI: −1.0, −0.2 MPa, P=0.017). There were no other significant changes in average contact stress on the labrum. Contact area on the labrum did not change on a regional basis when considering all activities (Fig. 6-B). Additionally, the change in percent load supported by the labrum from 10.8% pre- to 12.1% post-operatively was not significant when considering all activities (Fig. 6-C) (1.3%, 95% CI: −2.2, 4.7%, P=0.487).

Discussion

Using patient-specific FE models, we found that PAO shifted cartilage contact stress from more focal patterns anterolaterally to more diffuse stresses medially and superiorly, and reduced average and peak cartilage contact stress, thus confirming our first hypothesis. Only the total peak contact stress and average stress at the superior region of the labrum decreased significantly; labral load was not reduced. Therefore, our second hypothesis was not universally confirmed.

Reductions in cartilage contact stress may be necessary to prevent OA following PAO as chronic exposure to static compression ex-vivo has been shown to damage cartilage [40]. Medialization of the joint may also be required so as to minimize loading to focal cartilage lesions, subchondral cysts, and cartilage delaminations, which are often observed in the anterolateral acetabulum in dysplastic hips prior to PAO [12]. We found that cartilage contact area increased the most medially following PAO, with large reductions in contact stress at the anterior and lateral regions. Therefore, PAO may be efficacious at redistributing cartilage contact away from areas where damage is frequently observed in patients who are candidates for PAO.

By including patient-specific anatomy, we demonstrated that PAO reduces cartilage stresses primarily by redistributing contact, rather than by increasing the total contact area. Our findings are important as they suggest surgeons should not assume that an increase in femoral head coverage will yield a proportional reduction in contact stress. Considering that

total contact area to the cartilage was only increased by 4%, it was initially surprising to observe disproportionally larger reductions in cartilage stress following PAO. That is, if contact stress is defined as force divided by unit area, one could anticipate a linear relationship between coverage and stress. However, there are factors intrinsic to patient-specific FE hip models, such as the degree in which bones dissipate energy, the congruency of the joint, and the location in which contact occurs, that can make the interpretation of contact stress, contact area, and applied force non-intuitive. For example, following PAO, the orientation of the acetabulum was lateralized, which medialized acetabular cartilage contact stress; this enabled the acetabular bone to dissipate more energy, reducing contact stresses despite having identical forces applied across operative states. The hip is not spherical in dysplastic patients [41], and thus, rotation of the socket via PAO likely alters the congruency of the contacting interfaces. Even minor deviations from a congruent joint have been shown to induce areas of high (or low) contact stress [23]. The congruency of the joint also dictates where contact occurs. The acetabular roof may be rotated via PAO into a position that yields greater contact within the superior acetabulum. The roof is roughly aligned perpendicular to the direction of the applied joint reaction force, and thus, may dissipate energy more effectively, reducing cartilage contact stress.

Over-correction of PAO is believed to shift contact excessively medial, resulting in iatrogenic femoroacetabular impingement [42]. With elevated stress on the medial wall of the acetabulum, cartilage may become overloaded, and result in damage typically seen in patients with acetabular protrusio [43, 44]. One patient (PT 4, Fig. 3) demonstrated what may be excessive medial contact during WM; the FE model of this patient was also the only to report increased average contact stress on acetabular cartilage post-operatively. Surprisingly, this patient had a post-operative CEA within the normal range at 28.5°. Collectively, this suggests that it may be difficult to determine the appropriate degree of acetabular reorientation based on radiographic evaluation alone.

Although the stated goal of PAO is to reduce cartilage stresses, medialization of contact could reduce contact stress, contact area, and load to the labrum, especially in the superior region given that the majority of the hip joint reaction force acts in the superior direction [36]. We found a slight, but significant decrease in contact area of the superior labrum, with a corresponding significant decrease in average contact stress, suggesting that labral contact mechanics are improved in the superior region. However, the labrum supported 7.8 – 12.6% of the total hip joint reaction force pre-operatively to 8.6 – 15.5% post-operatively, which are both similar to data reported by Henak et al. for untreated dysplastic hips (~10%) [13]. Importantly, percent loads supported post-operatively remained 2–4 times higher than normal hips [13, 14]. We suspect that the excessively prominent, hypertrophied labrum of dysplastic hips remains in contact despite reorientation of the acetabulum, causing this tissue to continue to experience excessive load sharing. Although the clinical implications of achieving only modest improvements in labral contact mechanics following PAO are unknown, it has been suggested that abnormal labral mechanics leads to an outward-to-in progression of OA in dysplastic hips [13]; the pathogenesis of OA following PAO may occur in a similar fashion.

Only one prior study used patient-specific FE models to estimate cartilage contact mechanics in untreated dysplastic hips. Peak cartilage contact stresses estimated by Henak et al. (~12–15 MPa) were less than those reported in our study (~20 MPa). However, Henak averaged peak contact stress over six anatomical regions (see Supplemental Figure 1 by Henak et. al [13]); this approach likely reduced the peak stress reported for each region since the location of peak stress was different between patients. Average stresses predicted by Henak (~0.5–1.5 MPa) were also less than our values (~4 MPa). This difference is attributed to the fact that Henak considered all FE nodes on the articulating surface of the acetabular cartilage, even those nodes not in contact, when calculating the average.

Simplified models have been used to compare cartilage contact mechanics in pre- and post-operative states. Zhao et al. altered the geometry of a normal hip to simulate dysplasia and modeled varying degrees of acetabular reorientation to estimate the effects of PAO using FE analysis [22]. Armiger et al. used discrete element analysis to predict acetabular contact stress and contact area before and after PAO when assuming constant cartilage thickness and rigid (i.e. non-deformable) bones [28]. These simplified modeling studies had similar conclusions to ours: that PAO shifts contact medially and reduces cartilage contact stress. However, use of constant cartilage thickness is known to predict much larger contact areas with diffuse contact patterns [23]. As a result, the magnitude of contact stress and contact area predicted by our patient-specific FE models did not agree with data from the studies by Zhao and Armiger. For example, contact area reported by Armiger et al. averaged 1,559 ± 460 mm^2 and 2,337 ± 451 mm^2 pre- and post-operatively, respectively, which are ~5 times larger than our results. It is important to note that Armiger's estimates of contact area were nearly 4 times larger compared to other subject- and patient-specific hip FE models developed from a validated pipeline [13, 19, 20, 25, 27]. Therefore, estimates of cartilage contact mechanics from models that do not incorporate patient- specific anatomy for cartilage and bone should be interpreted with caution. We cannot compare labral contact mechanics estimated in our study to work by Armiger and Zhao, as they did not include the labrum in their models.

There are several limitations to our study. We reported cartilage contact stress, as this variable has frequently been implicated as the cause of damage and increased rates of OA in dysplastic hips [45–48]. However, deleterious shear stresses may play a role in the pathogenesis of OA [5]. Unfortunately, to our knowledge, investigators have yet to demonstrate that FE models of the hip can accurately predict shear stress. In the absence of these validation data, and given the previously established relationship between elevated contact stress and the development of OA in dysplastic hips [45–48], we believed it was both prudent and reasonable to report only contact stress and contact area. An additional limitation was that the time-intensive process to generate and analyze patient-specific FE models both pre- and post-surgery along with the need for repeated CT scans prohibited use of a large sample size. Yet, having patients serve as their own control strengthened the statistical analysis. Also, follow-up time was an average of 19 months; bone and/or cartilage remodeling may occur over a period of longer follow-up. Moreover, patients with dysplasia have been noted to have altered gait patterns [49, 50], which may or may not remain altered following surgery [51, 52]. However, we applied identical kinematics in pre- and post-operative states. By using identical loading and boundary conditions, we were able to focus

on how altering hip morphology as a result of PAO influenced chondrolabral mechanics. It would have otherwise been difficult to isolate the mechanical importance of morphological changes that follow PAO if patient-specific boundary and loading conditions were implemented. In this regard, boundary and loading conditions were based on data from older patients with instrumented total hip replacements [36]. Incorporating hip kinematics and joint reaction forces specific to patients with dysplasia could alter FE predictions, but we suspect that this change would not be pronounced. Specifically, a previous FE modeling study of hip dysplasia showed that changes in the kinematic position and magnitude of the applied joint reaction force did not impose major changes in labral loading [14]. Another possible limitation is that errors in the representation of FE model geometry could influence predictions. Our method of semi-automatic segmentation yields a reconstruction error less than 10% for representing cartilage [29] and the thickness of the cortex [30]. Previous validation studies indicated that models developed using this semi-automatic segmentation technique accurately predict hip contact mechanics [19, 20]. Patients had screws in their hips at the time of the post-operative CT. Metal artifact was minimal, and thus, we do not believe it affected the accuracy of our segmentation. Screws were located some distance away from the acetabulum, and the osteotomy site had healed completely in all patients, and thus inclusion of screws would have minimal impact on FE predictions. Concomitant deformities to the femoral head are common in hips with dysplasia [7, 41]. Our criteria for selecting subjects were based on the CEA and acetabular index in the coronal plane. Thus, we did not screen subjects based on the radiographic appearance of their femur.

Cartilage was represented as a hyperelastic material, which is a simplification of the actual behavior [20, 27, 33]. However, use of this constitutive model does not alter cartilage contact stresses substantially compared to more sophisticated representations [20]. The effects of poroelasticity were excluded when modeling cartilage and labrum. However, based on the permeability of these tissues, one would expect minimal fluid exudation at loading rates consistent with gait [35, 53]. Despite the purported sealing role of the labrum [54–57], there is no direct evidence that labral sealing influences chondrolabral contact mechanics [14]. Material properties for the labrum were derived from bovine, not human tissue. Labra of patients with dysplasia may become calcified due to repetitive loading, and thus, assuming material properties based on non-pathologic tissue (bovine or human) may inaccurately represent labral mechanics. To our knowledge, the information necessary to define dysplasia-specific material coefficients for the purpose of representing the labrum as a transversely isotropic hyperelastic material is not available. Fortunately, FE predictions are insensitive to changes in labral properties (e.g. altering the fiber stiffness by ±50% only changes labrum load support by 0–1% [14]).

In conclusion, our results indicate PAO was efficacious at medializing cartilage contact and reducing cartilage contact stresses, and therefore may minimize loading to focal cartilage lesions and subchondral cysts often observed in the lateral acetabulum of dysplastic hips. However, the excessively prominent, hypertrophied labrum of dysplastic hips may remain in contact with the femoral head following PAO, which may explain why load to the labrum remained 2–4 times higher in treated patients than normal hips. A longer follow-up of these patients could provide insight into the role of acetabular labrum in the pathogenesis of OA following PAO.

Acknowledgements

Financial support was provided by the National Institutes of Health (NIH) R01-AR053344, R01- GM083925, R01-EB016701, R21-AR3466184, 5UL1TR001067, and the LS-Peery Discovery Program in Musculoskeletal Restoration.

Role of Funding Source

Funding was provided by the NIH and the LS-Peery Discovery Program in Musculoskeletal Restoration. The research content herein is solely the responsibility of the authors and does not necessarily represent the official views of the National Institutes of Health or LS-Peery Foundation.

References

1. Murphy NJ, Eyles JP, Hunter DJ. Hip Osteoarthritis: Etiopathogenesis and Implications for Management. Adv Ther 2016; 33: 1921–1946. [PubMed: 27671326]
2. Clohisy JC, Dobson MA, Robison JF, Warth LC, Zheng J, Liu SS, et al. Radiographic structural abnormalities associated with premature, natural hip-joint failure. J Bone Joint Surg Am 2011; 93 Suppl 2: 3–9. [PubMed: 21543681]
3. Jacobsen S, Sonne-Holm S. Hip dysplasia: a significant risk factor for the development of hip osteoarthritis. A cross-sectional survey. Rheumatology 2005; 44: 211–218. [PubMed: 15479751]
4. Barros HJ, Camanho GL, Bernabe AC, Rodrigues MB, Leme LE. Femoral head-neck junction deformity is related to osteoarthritis of the hip. Clin Orthop Relat Res 2010; 468: 1920–1925. [PubMed: 20352385]
5. Smith RL, Carter DR, Schurman DJ. Pressure and shear differentially alter human articular chondrocyte metabolism: a review. Clin Orthop Relat Res 2004: S89–95. [PubMed: 15480081]
6. Nunley RM, Prather H, Hunt D, Schoenecker PL, Clohisy JC. Clinical presentation of symptomatic acetabular dysplasia in skeletally mature patients. J Bone Joint Surg Am 2011; 93 Suppl 2: 17–21. [PubMed: 21543683]
7. Kosuge D, Yamada N, Azegami S, Achan P, Ramachandran M. Management of developmental dysplasia of the hip in young adults: current concepts. The bone & joint journal 2013; 95-B: 732–737. [PubMed: 23723265]
8. Leunig M, Siebenrock KA, Ganz R. Rationale of periacetabular osteotomy and background work. Instructional course lectures 2001; 50: 229–238. [PubMed: 11372318]
9. Russell ME, Shivanna KH, Grosland NM, Pedersen DR. Cartilage contact pressure elevations in dysplastic hips: a chronic overload model. J Orthop Surg Res 2006; 1: 6. [PubMed: 17150126]
10. Ganz R, Klaue K, Vinh TS, Mast JW. A new periacetabular osteotomy for the treatment of hip dysplasias. Technique and preliminary results. Clin Orthop Relat Res 1988: 26–36.
11. Tibor LM, Sink EL. Periacetabular osteotomy for hip preservation. The Orthopedic clinics of North America 2012; 43: 343–357. [PubMed: 22819162]
12. Domb B, LaReau J, Redmond JM. Combined hip arthroscopy and periacetabular osteotomy: indications, advantages, technique, and complications. Arthroscopy techniques 2014; 3: e95–e100. [PubMed: 24843847]
13. Henak CR, Abraham CL, Anderson AE, Maas SA, Ellis BJ, Peters CL, et al. Patient-specific analysis of cartilage and labrum mechanics in human hips with acetabular dysplasia. Osteoarthritis and Cartilage 2014; 22: 210–217. [PubMed: 24269633]
14. Henak CR, Ellis BJ, Harris MD, Anderson AE, Peters CL, Weiss JA. Role of the acetabular labrum in load support across the hip joint. J Biomech 2011; 44: 2201–2206. [PubMed: 21757198]
15. Hartig-Andreasen C, Troelsen A, Thillemann TM, Soballe K. What factors predict failure 4 to 12 years after periacetabular osteotomy? Clin Orthop Relat Res 2012; 470: 2978–2987. [PubMed: 22576934]
16. Matheney T, Kim YJ, Zurakowski D, Matero C, Millis M. Intermediate to long-term results following the Bernese periacetabular osteotomy and predictors of clinical outcome. J Bone Joint Surg Am 2009; 91: 2113–2123. [PubMed: 19723987]

17. McKinley TO. The Bernese periacetabular osteotomy for treatment of adult hip dysplasia. Skel Rad 2010; 39: 1057–1059.
18. Steppacher SD, Tannast M, Ganz R, Siebenrock KA. Mean 20-year followup of Bernese periacetabular osteotomy. Clin Orthop Relat Res 2008; 466: 1633–1644. [PubMed: 18449617]
19. Anderson AE, Ellis BJ, Maas SA, Peters CL, Weiss JA. Validation of finite element predictions of cartilage contact pressure in the human hip joint. J Biomech Eng 2008; 130: 051008. [PubMed: 19045515]
20. Henak CR, Kapron AL, Anderson AE, Ellis BJ, Maas SA, Weiss JA. Specimen-specific predictions of contact stress under physiological loading in the human hip: validation and sensitivity studies. Biomechanics and modeling in mechanobiology 2014; 13: 387–400. [PubMed: 23736783]
21. Henak CR, Anderson AE, Weiss JA. Subject-specific analysis of joint contact mechanics: application to the study of osteoarthritis and surgical planning. J Biomech Eng 2013; 135: 021003. [PubMed: 23445048]
22. Zhao X, Chosa E, Totoribe K, Deng G. Effect of periacetabular osteotomy for acetabular dysplasia clarified by three-dimensional finite element analysis. J Orthop Sci 2010; 15: 632–640. [PubMed: 20953924]
23. Anderson AE, Ellis BJ, Maas SA, Weiss JA. Effects of idealized joint geometry on finite element predictions of cartilage contact stresses in the hip. J Biomech 2010; 43: 1351–1357. [PubMed: 20176359]
24. Gu DY, Hu F, Wei JH, Dai KR, Chen YZ. Contributions of non-spherical hip joint cartilage surface to hip joint contact stress. Annual International Conference of the IEEE Engineering in Medicine and Biology Society. 2011; 2011: 8166–8169.
25. Harris MD, Anderson AE, Henak CR, Ellis BJ, Peters CL, Weiss JA. Finite element prediction of cartilage contact stresses in normal human hips. J Orthop Res 2012; 30: 1133–1139. [PubMed: 22213112]
26. Henak CR, Abraham CL, Peters CL, Sanders RK, Weiss JA, Anderson AE. Computed tomography arthrography with traction in the human hip for three-dimensional reconstruction of cartilage and the acetabular labrum. Clin Radiol 2014; 69: e381–391. [PubMed: 25070373]
27. Henak CR, Carruth ED, Anderson AE, Harris MD, Ellis BJ, Peters CL, et al. Finite element predictions of cartilage contact mechanics in hips with retroverted acetabula. Osteoarthritis and Cartilage 2013; 21: 1522–1529. [PubMed: 23792188]
28. Armiger RS, Armand M, Tallroth K, Lepisto J, Mears SC. Three-dimensional mechanical evaluation of joint contact pressure in 12 periacetabular osteotomy patients with 10-year follow-up. Acta Orthop 2009; 80: 155–161. [PubMed: 19404795]
29. Anderson AE, Ellis BJ, Peters CL, Weiss JA. Cartilage thickness: factors influencing multidetector CT measurements in a phantom study. Radiology 2008; 246: 133–141. [PubMed: 18096534]
30. Anderson AE, Peters CL, Tuttle BD, Weiss JA. Subject-specific finite element model of the pelvis: development, validation and sensitivity studies. J Biomech Eng 2005; 127: 364–373. [PubMed: 16060343]
31. Dalstra M, Huiskes R. Load transfer across the pelvic bone. J Biomech 1995; 28: 715–724. [PubMed: 7601870]
32. Park S, Hung CT, Ateshian GA. Mechanical response of bovine articular cartilage under dynamic unconfined compression loading at physiological stress levels. Osteoarthritis and Cartilage 2004; 12: 65–73. [PubMed: 14697684]
33. Mow VC, Huiskes R. Basic orthopaedic biomechanics & mechano-biology, Lippincott Williams & Wilkins 2005.
34. Quapp KM, Weiss JA. Material characterization of human medial collateral ligament. J Biomech Eng 1998; 120: 757–763. [PubMed: 10412460]
35. Ferguson SJ, Bryant JT, Ito K. The material properties of the bovine acetabular labrum. J Orthop Res 2001; 19: 887–896. [PubMed: 11562138]
36. Bergmann G, Deuretzbacher G, Heller M, Graichen F, Rohlmann A, Strauss J, et al. Hip contact forces and gait patterns from routine activities. J Biomech 2001; 34: 859–871. [PubMed: 11410170]

37. Puso MA, Maker BN, Ferencz RM, Hallquist JO. NIKE3D: A Nonlinear, Implicit, Three-Dimensional Finite Element Code for Solid and Structural Mechanics. User's Manual. 2007.
38. Maas SA, Ellis BJ, Ateshian GA, Weiss JA. FEBio: finite elements for biomechanics. J Biomech Eng 2012; 134: 011005. [PubMed: 22482660]
39. Finner H On a Monotonicity Problem in Step-Down Multiple Test Procedures. Journal of the American Statistical Association 1993; 88: 920–923.
40. Guilak F, Fermor B, Keefe FJ, Kraus VB, Olson SA, Pisetsky DS, et al. The role of biomechanics and inflammation in cartilage injury and repair. Clin Orthop Relat Res 2004: 17–26.
41. Steppacher SD, Tannast M, Werlen S, Siebenrock KA. Femoral morphology differs between deficient and excessive acetabular coverage. Clin Orthop Relat Res 2008; 466: 782–790. [PubMed: 18288550]
42. Turgeon TR, Phillips W, Kantor SR, Santore RF. The role of acetabular and femoral osteotomies in reconstructive surgery of the hip: 2005 and beyond. Clin Orthop Relat Res 2005; 441: 188–199. [PubMed: 16331002]
43. Crowninshield RD, Brand RA, Pedersen DR. A stress analysis of acetabular reconstruction in protrusio acetabuli. J Bone Joint Surg Am 1983; 65: 495–499. [PubMed: 6833325]
44. Leunig M, Nho SJ, Turchetto L, Ganz R. Protrusio acetabuli: new insights and experience with joint preservation. Clin Orthop Relat Res 2009; 467: 2241–2250. [PubMed: 19408062]
45. Hadley NA, Brown TD, Weinstein SL The effect of contact pressure elevations and aseptic necrosis on long term outcome of congenital hip dislocation. J Orthop Res 1990; 8: 504–510. [PubMed: 2355290]
46. Maxian TA, Brown TD, Weinstein SL. Chronic stress tolerance levels for human articular cartilage: two nonuniform contact models applied to long-term follow-up of CDH. J Biomech 1995; 28: 159–166. [PubMed: 7896858]
47. Hipp JA, Sugano N, Millis MB, Murphy SB. Planning acetabular redirection osteotomies based on joint contact pressures. Clin Orthop 1999: 134–143. [PubMed: 10416402]
48. Michaeli DA, Murphy SB, Hipp JA. Comparison of predicted and measured contact pressures in normal and dysplastic hips. Med Eng Phys 1997; 19: 180–186. [PubMed: 9203153]
49. Jacobsen JS, Nielsen DB, Sorensen H, Soballe K, Mechlenburg I. Changes in walking and running in patients with hip dysplasia. Acta Orthop 2013; 84: 265–270. [PubMed: 23594221]
50. Romano CL, Frigo C, Randelli G, Pedotti A. Analysis of the gait of adults who had residua of congenital dysplasia of the hip. J Bone Joint Surg Am 1996; 78: 1468–1479. [PubMed: 8876573]
51. Endo H, Mitani S, Senda M, Kawai A, McCown C, Umeda M, et al. Three-dimensional gait analysis of adults with hip dysplasia after rotational acetabular osteotomy. J Orthop Sci 2003; 8: 762–771. [PubMed: 14648262]
52. Pedersen EN, Alkjaer T, Soballe K, Simonsen EB. Walking pattern in 9 women with hip dysplasia 18 months after periacetabular osteotomy. Acta Orthop 2006; 77: 203–208. [PubMed: 16752280]
53. Ateshian GA, Ellis BJ, Weiss JA. Equivalence between short-time biphasic and incompressible elastic material responses. J Biomech Eng 2007; 129: 405–412. [PubMed: 17536908]
54. Ferguson SJ, Bryant JT, Ganz R, Ito K. The acetabular labrum seal: a poroelastic finite element model. Clin Biomech 2000; 15: 463–468.
55. Ferguson SJ, Bryant JT, Ganz R, Ito K. The influence of the acetabular labrum on hip joint cartilage consolidation: a poroelastic finite element model. J Biomech 2000; 33: 953–960. [PubMed: 10828325]
56. Ferguson SJ, Bryant JT, Ganz R, Ito K. An in vitro investigation of the acetabular labral seal in hip joint mechanics. J Biomech 2003; 36: 171–178. [PubMed: 12547354]
57. Hlavacek M The influence of the acetabular labrum seal, intact articular superficial zone and synovial fluid thixotropy on squeeze-film lubrication of a spherical synovial joint. J Biomech 2002; 35: 1325–1335. [PubMed: 12231278]

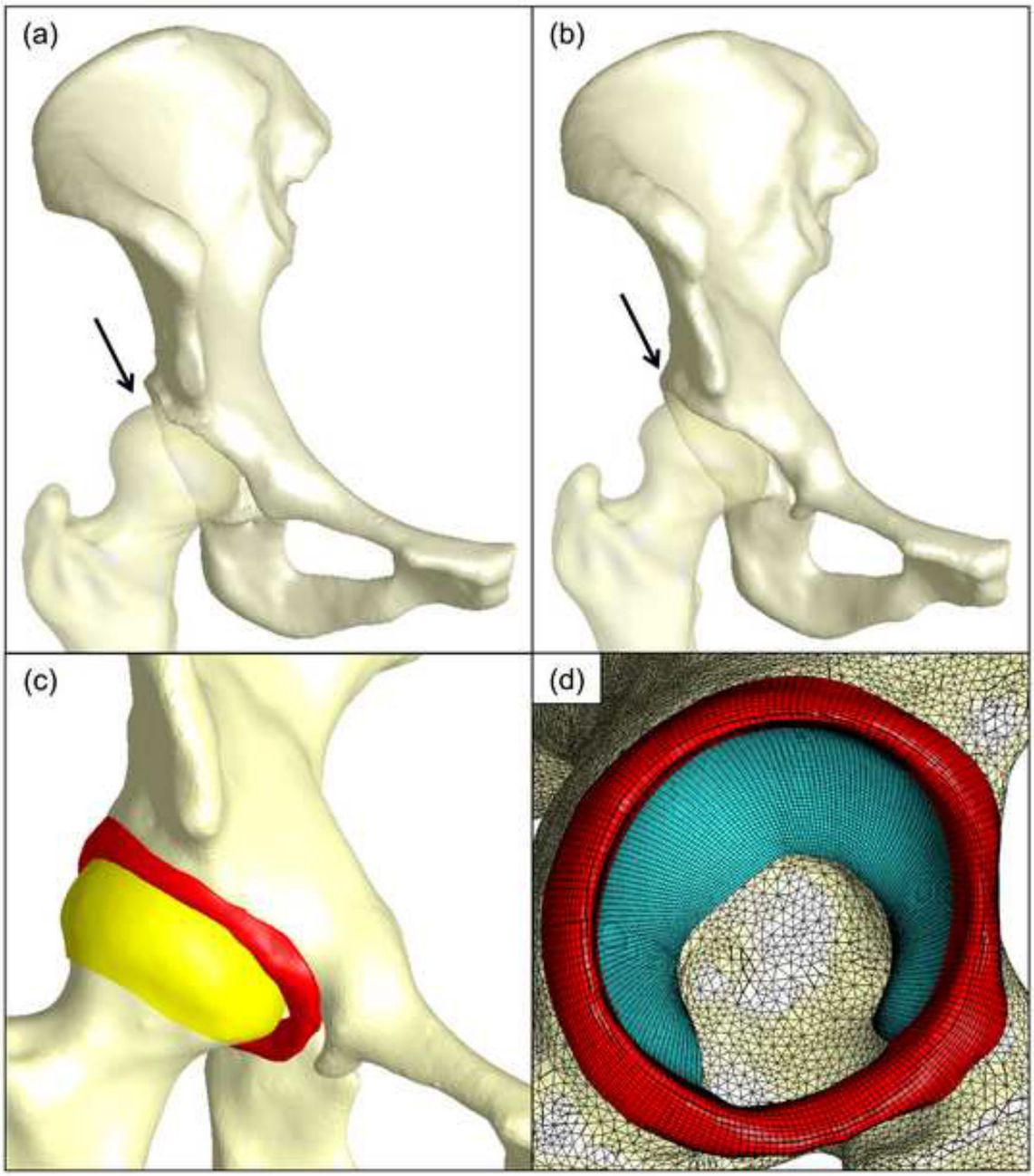

Figure 1.

Finite element model representation for a single patient. Patient-specific 3D reconstructions of the femur and pelvis in the (a) pre-operative and (b) post-operative state. The femurs are semitransparent to highlight anterolateral femoral coverage (indicated by the arrows). (c) Representative post-operative model showing bone, femoral cartilage, and labrum. (d) Sagittal view of mesh discretization for bone (yellow) acetabular cartilage (blue) and labrum (red).

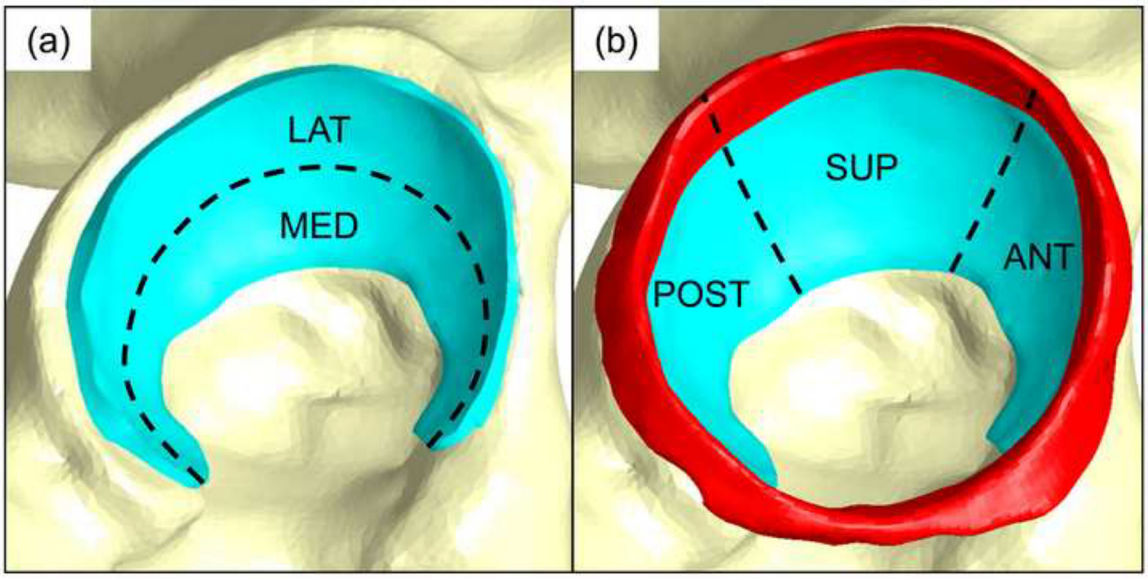

Figure 2.
Regions of acetabular cartilage and labrum analyzed. (a) Lateral and medial regions were analyzed for acetabular cartilage. (b) A three-region analysis then partitioned acetabular cartilage (blue) and labrum (red) into anterior, superior, and posterior regions.

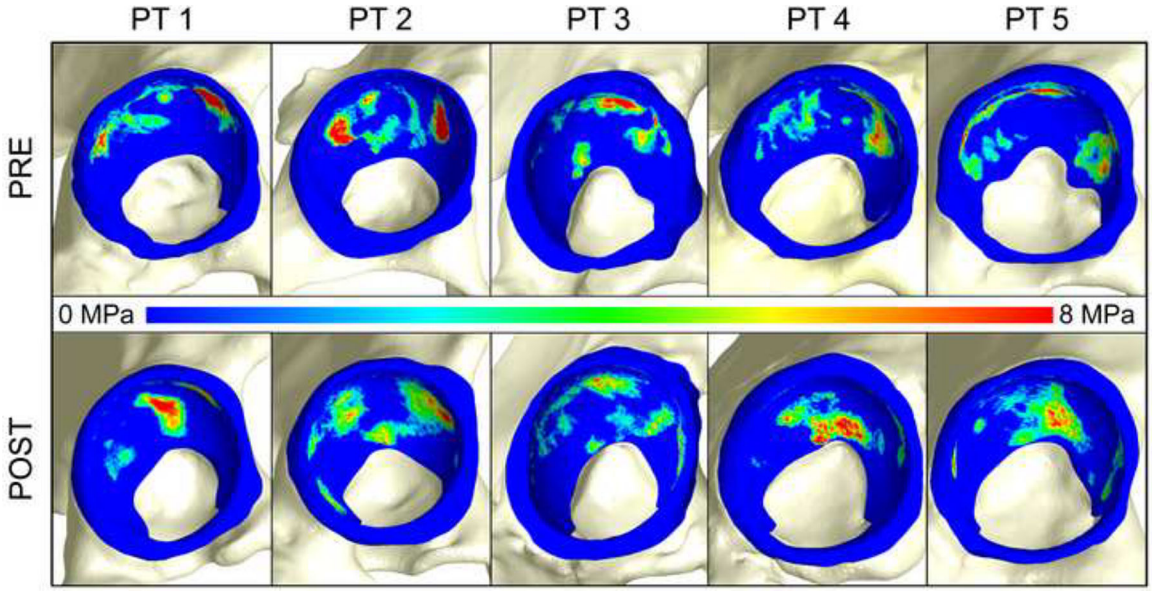

Figure 3.

Contact stress (a) pre- and (b) post-operatively for walking at midstance for each patient (PT). In general, contact was better distributed post-operatively with stress medialized. However, for one patient (PT 4), higher stresses were observed on the medial portion of the acetabulum, extending to the acetabular fossa. Note – the fringe scale has been set to a maximum of 8 MPa to show areas of elevated contact stress. However, peak contact stresses often exceeded 8 MPa.

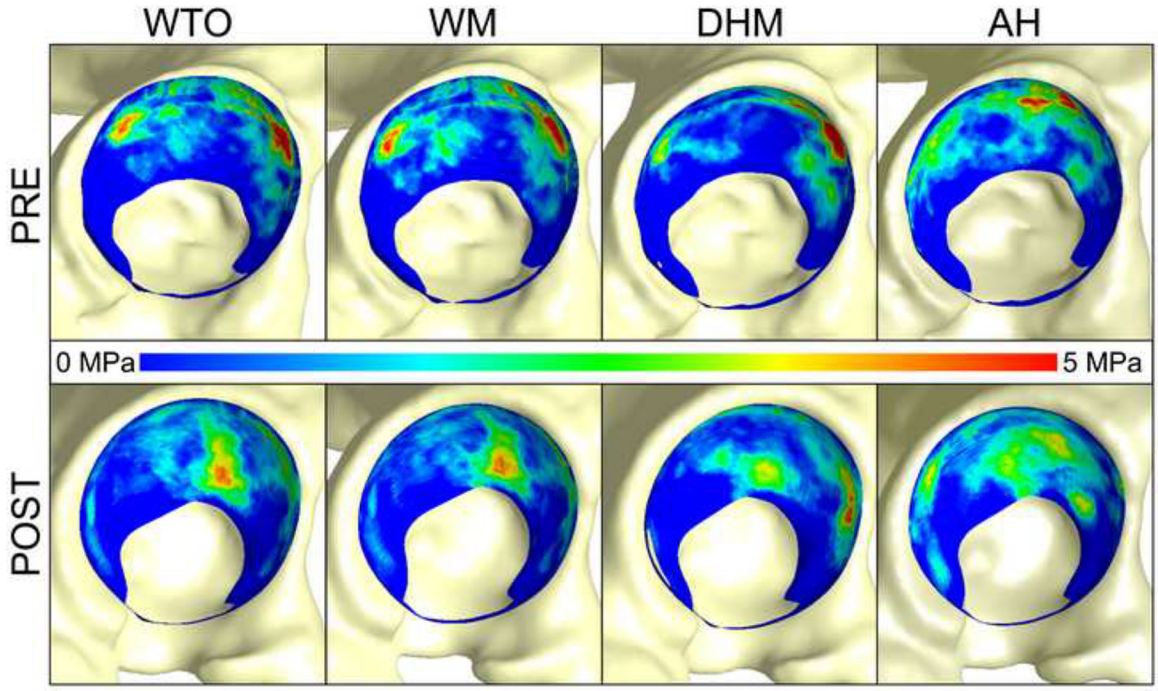

Figure 4.

Average contact stress of all five patients pre- (top row) and post-operatively (bottom row) during all activities. Contact shifted medially for all patients post-operatively. Anterolateral focal loading was alleviated post-operatively. Note: contact stresses from all five subjects have been mapped to a single mesh for visualization. The labrum is not shown.

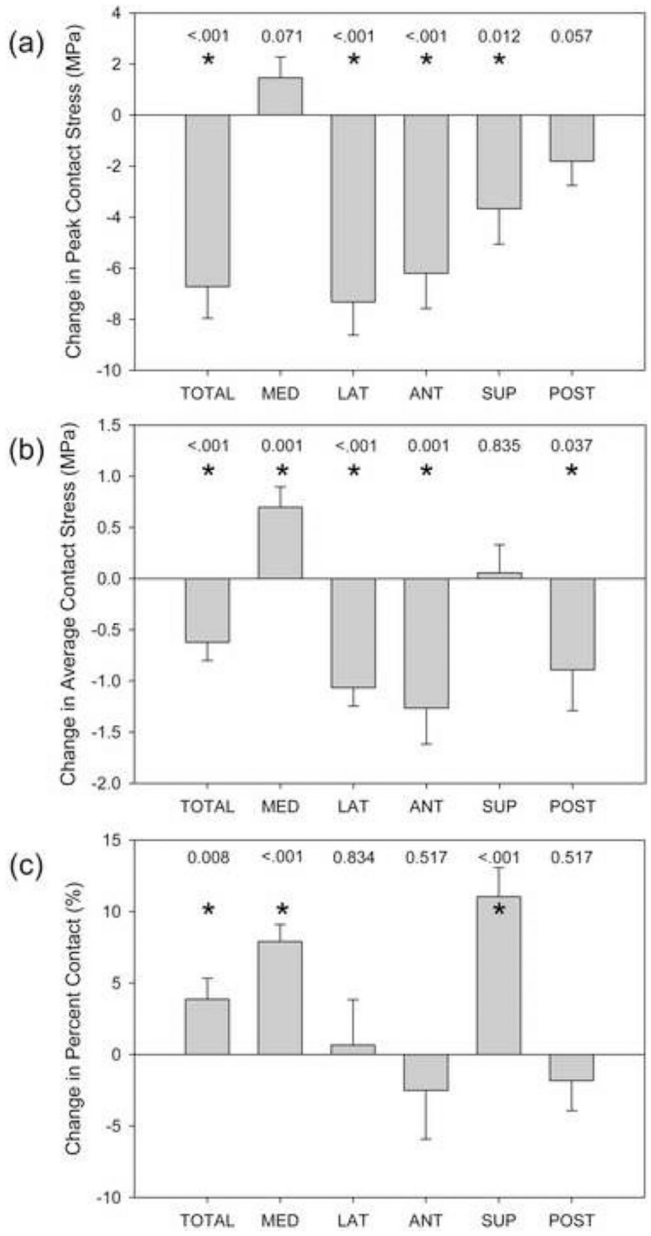

Figure 5.

Post-operative changes in acetabular cartilage mechanics. (a) Peak contact stress significantly decreased overall, and in the lateral, anterior, and superior regions. (b) Average contact stress was significantly reduced overall, and in the lateral, anterior, and posterior regions; average contact stress increased medially. (c) Percent contact area significantly increased overall, and in the medial and superior regions. Bars indicate standard error. P values are listed and * indicates $P \leq 0.05$.

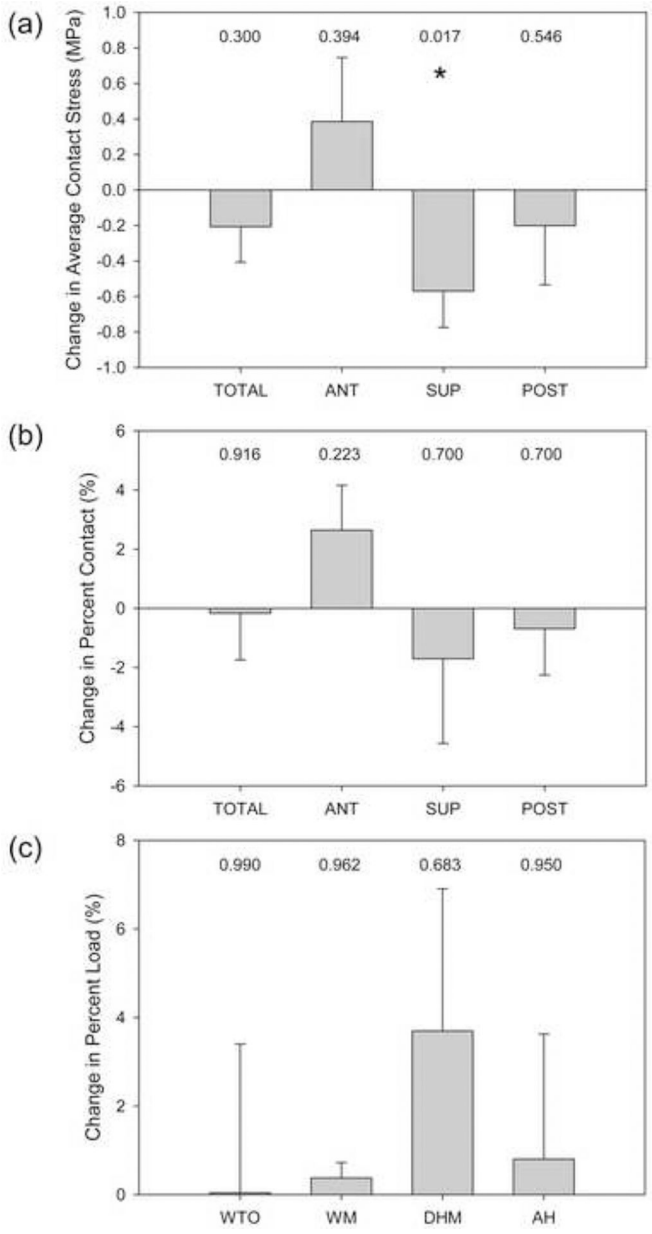

Figure 6.

Post-operative changes in labral mechanics. (a) Average contact stress significantly decreased in the superior region only. There were no significant changes in (b) percent contact or (c) percent load supported by the labrum. Bars indicate standard error. P values are listed and * indicates $P \leq 0.05$.